



Castor–babassu biodiesel blends: estimating kinetic parameters by Differential Scanning Calorimetry using the Borchardt and Daniels method

Rubem S. F. Paula¹ · Igor M. Figueredo^{1,3} · Rodrigo S. Vieira¹ · Tassio L. Nascimento² · Célio L. Cavalcante Jr.¹ · Yguatyrara L. Machado³ · Maria A. S. Rios³

© Springer Nature Switzerland AG 2019

Abstract

The main objective of this study was to assess the kinetics of the deterioration of blends of babassu and castor biodiesel. The biodiesel samples were synthesized by catalytic transesterification and characterized for their main physical properties such as kinematic viscosity, density, acid number, ester content, and oxidation stability. Thermal profiles were carried out using the Differential Scanning Calorimetry technique as presented in the American Society for Testing and Materials (ASTM) E537 standard. Kinetic parameters were obtained using ASTM E2041 standard (Borchardt–Daniels method), following a statistical treatment from the ASTM E1970 standard. Among all samples, the pure castor biodiesel sample showed the highest extrapolated onset temperature (T_s), 214.92 °C, and lowest reaction rate [$k(T)$], $1.02 \times 10^{-3} \text{ min}^{-1}$, indicating that this sample is more resistant to oxidation. On the other hand, the blend with the babassu/castor biodiesel mass ratio of 75/25 was the most prone to oxidize. Thus, castor biodiesel may be used as an additive to improve the oxidative stability of other sources of biodiesel, including babassu biodiesel.

Keywords Babassu biodiesel · Castor biodiesel · Differential Scanning Calorimetry · Kinetic parameters

1 Introduction

Renewable energy sources have been intensely studied in Brazil and overseas. Focusing on sustainable development, researchers have been investigating new sources of clean energy, which may contribute to decreasing environmental impacts [1–3]. According to data from the 2017 Brazilian Energy Balance, 41.5% of all energy produced in Brazil come from renewable resources, namely biomass (25.0%) and hydroelectric plants (11.1%). The other sources are petroleum (44.2%), natural gas (12.8%) and mineral coal (0.9%) [4].

In this context, biodiesel becomes an important bio-fuel option. The production of biodiesel provides new job opportunities for both the rural workforce and specialized workers in the industrial sector. The use of this biofuel also contributes to the reduction of environmental pollution levels, since it does not contain sulfur or aromatic compounds. Particulates and gas emissions, such as HC, CO, and CO₂, are also lower. Additionally, biodiesel is non-toxic, biodegradable, and produced using renewable sources [1–3, 5–7].

However, biodiesel presents some disadvantages compared to mineral diesel. The major problem is the cost of production: biodiesel is, by far, more expensive

✉ Maria A. S. Rios, alexsandrarios@ufc.br | ¹Departamento de Engenharia Química, Grupo de Pesquisa em Separações por Adsorção, Núcleo de Pesquisas em Lubrificantes, Universidade Federal do Ceará, Campus do Pici, Bl. 709, Fortaleza, CE 60.455-900, Brazil. ²Instituto Federal de Educação, Ciência e Tecnologia do Ceará, Campus Tabuleiro do Norte, Rodovia CE 377, Km 2- Sítio Taperinha, Tabuleiro do Norte, CE 62960-000, Brazil. ³Departamento de Engenharia Mecânica, Grupo de Inovações Tecnológicas e Especialidades Químicas, Universidade Federal do Ceará, Campus do Pici, Bl. 714, Fortaleza, CE 60.440-554, Brazil.



than mineral diesel, mainly because of the high cost of raw materials (about 60–75% of the final biofuels price) [2, 3]. The use of new routes and technology may become this process cheaper than nowadays. For instance, Hajilari et al. [3] reported the use of membrane processes to improve the quality of the biofuels, adding value to the final products.

Biodiesel is formed by long-chain alkyl esters of carboxylic acids, produced through transesterification and/or esterification of a fatty substance from vegetable oils or animal fats. This biofuel may be produced from a variety of sources, including castor oil, soy oil, sunflower oil, babassu oil, beef tallow, fish oil, and others [8, 9]. Since it is obtained from organic matter and includes polyunsaturated esters in its chemical structure, biodiesel is susceptible to oxidation at temperatures as low as 110 °C [10]. In the current study, we assessed the thermal deterioration of biodiesel blends derived from castor and babassu oils in various blending ratios (0–100%) using the Differential Scanning Calorimetry (DSC) technique.

Some studies have described the use of DSC equipment and the Borchardt–Daniels method to assess the oxidation reaction of different samples [11, 12]. Fryer and Taylor [11] evaluated the reaction kinetics of whey proteins using that method. However, due to whey protein characteristics, the Borchardt–Daniels method was inappropriate for this case. On the other hand, Kok et al. [12] used P-DSC (DSC with controlled pressure) to evaluate the kinetic behavior of two crude oils, varying the pressure in a programmed temperature range. In this case, the Borchardt–Daniels method provided suitable results.

In addition, the determination of kinetic parameters of the oxidation reaction of the vegetable oils has already been reported in some studies, such as Thurgood et al. [13] and Micic et al. [14]. Both studies reported that the reaction rate, $k(T)$, is the main kinetic parameter to evaluate the oxidation reaction. In other words, if one sample

presents higher $k(T)$ values than others, that sample is more prone to oxidize.

The current study aims to assess the kinetic deterioration of biodiesel samples produced by two important oleaginous plants of the Brazilian Northeast region, castor (*Ricinus communis* L.) and babassu (*Orbignya* sp.) oils. Babassu and castor biodiesel samples (BB and CB, respectively) were blended in mass ratios of 0/100, 25/75, 50/50, 75/25 and 100/0 (CB/BB). The kinetic deterioration was then assessed using the DSC technique (ASTM E537 standard and Borchardt–Daniels method) in an oxidizing atmosphere in order to map their oxidation stabilities [15, 16].

2 Experimental section

2.1 Materials

The pure biodiesel samples (BB and CB) were synthesized by alkaline catalytic transesterification [5, 9, 17–20] and their main physicochemical properties (ester content, kinematic viscosity, density, acid number, and oxidation stability) are presented in Table 1. The BB/CB blends were prepared in mass ratios of 0/100, 25/75, 50/50, 75/25, and 100/0.

As mentioned before, biodiesel is obtained from a mixture of fatty acids. In this way, the castor oil biodiesel (CB) is mainly formed from ricinoleic acid, while the babassu oil biodiesel (BB) is mainly formed by saturated esters, especially the one from lauric acid. The different compositions and chemical structures of those fatty acids promote distinct physicochemical properties in the resulting biodiesel, including the oxidative stability [27, 28]. The chemical structures of these fatty acids are presented in Fig. 1.

The hydroxyl group (–OH) in the chemical structure of ricinoleic acid is (highlighted in Fig. 1) is the main factor for the high oxidation stability, kinematic viscosity, and cold

Table 1 Physicochemical properties of castor (CB) and babassu (BB) biodiesel samples

Sample	Property	Result	Specification ^a	Methods
Babassu biodiesel (BB)	Ester content	96.5%	96.5% min	EN 14103 [21]
	Kinematic viscosity (40 °C)	2.8	3.0–6.0 mm ² s ⁻¹	ASTM D7042 [22]
	Density (20 °C)	873	850–900 kg m ⁻³	ASTM D445 [23]
	Acid number	0.23	0.50 mg KOH g ⁻¹ max.	EN 14104 [24]
	Oxidation stability, induction period (110 °C)	5.43	8 h min	EN 14112 [25]
Castor biodiesel (CB)	Ester content	98.3%	96.5% min	EN 14103 [21]
	Kinematic viscosity (40 °C)	15.0	3.0–6.0 mm ² s ⁻¹	ASTM D7042 [22]
	Density (20 °C)	926	850–900 kg m ⁻³	ASTM D445 [23]
	Acid number	0.30	0.50 mg KOH g ⁻¹ max.	EN 14104 [24]
	Oxidation stability, induction period (110 °C)	14.74	8 h min	EN 14112 [25]

^aResolution ANP (Brazilian National Agency of Petroleum, Natural Gas and Biofuels) No. 45, of August 25, 2014 [26]

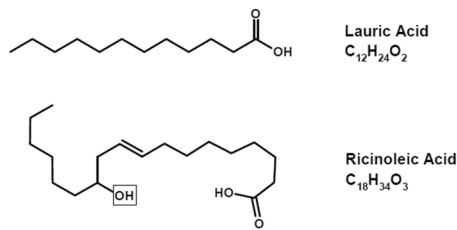


Fig. 1 Predominant fatty acids present in babassu oil (lauric) and castor oil (ricinoleic)

flow properties [29] of the biodiesel sample obtained from castor oil (CB).

2.2 Measurements

Samples of 5 ± 0.1 mg were evaluated using a DSC 1, with a Gas Controller GC 200 (both from Mettler Toledo; Columbus, Ohio, USA), in aluminum crucibles with synthetic air flowing at 50 mL min^{-1} . The temperature was increased from 30 to $500 \text{ }^\circ\text{C}$ at a heating rate, β , of $5 \text{ }^\circ\text{C min}^{-1}$. Calibration was performed using indium ($T_{\text{Melting Temperature}} = 429.75 \text{ K}$, $\Delta H_{\text{fusion}} = 28.54 \text{ J g}^{-1}$) and zinc ($T_{\text{Melting Temperature}} = 692.75 \text{ K}$, $\Delta H_{\text{fusion}} = 108.09 \text{ J g}^{-1}$) [30, 31]. The STARe Evaluation Software, provided by Mettler Toledo (Columbus, Ohio, USA), was used for the curves manipulation.

The enthalpy variation (ΔH), onset temperature (T_o), extrapolated onset temperature (T_s) and peak temperature (T_p) were obtained following ASTM E537: The Thermal Stability of Chemicals by Differential Scanning Calorimetry [15]. The reaction order, activation energy and Arrhenius pre-exponential factor were obtained following ASTM E2041: Estimating Kinetic Parameters by Differential Scanning Calorimeter Using the Borchardt and Daniels Method [16]. The Borchardt and Daniels method is applicable for temperatures between 170 and 870 K for exothermic reactions. The sample is heated at a linear rate and the rate of heat evolution, due to a chemical reaction, is proportional to the reaction rate. Integration of the heat flow as a function of time yields the total heat of a reaction [16].

2.3 Borchardt and Daniels method

Among several equations that drive kinetic models, the Borchardt and Daniels method uses two equations as a basis to determine their kinetic parameters. The first one is the rate equation to describe the dependence of the reaction rate on the amount of material present (Eq. 1).

$$\frac{d\alpha}{dt} = k(T)(1 - \alpha)^n \quad (1)$$

where da/dt = reaction rate (min^{-1}); $k(T)$ = rate constant at temperature T (min^{-1}); T = absolute temperature (K);

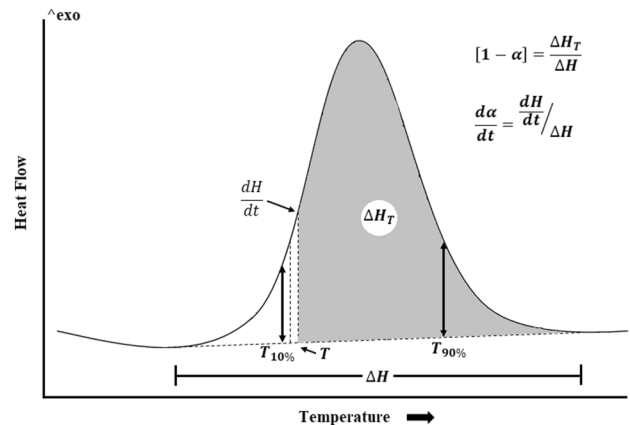


Fig. 2 Experimental data used to obtain kinetic parameters by the Borchardt and Daniels method

α = fraction reacted (dimensionless); and n = reaction order (dimensionless).

Second, the model also uses the Arrhenius equation (Eq. 2) to describe how the reaction rate changes as a function of temperature [15, 16].

$$\ln [k(T)] = \ln [Z] - \frac{E}{RT} \quad (2)$$

where Z = Arrhenius pre-exponential factor (min^{-1}); E = activation energy (J mol^{-1}); and R = gas constant ($= 8.314 \text{ J mol}^{-1} \text{ K}^{-1}$).

The experimental parameters are then evaluated using Eq. 3, which represents a combination between the logarithm forms of Eqs. 1 and 2.

$$\ln \left[\frac{d\alpha}{dt} \right] = \ln [Z] + n \ln [1 - \alpha] - \frac{E}{RT} \quad (3)$$

Equation 3 has the form of $z = a + bx + cy$,

Where $z \equiv \ln[da/dt]$; $a \equiv \ln[Z]$; $b \equiv n$; $x \equiv \ln[1 - \alpha]$; $c \equiv -E/T$; and $y \equiv 1/T$.

Multiple linear regression data treatment, ASTM E1970 [32], is used to solve Eq. 3. This standard requires the da/dt , $[1 - \alpha]$ and T values, which may be easily estimated from the exothermic reactions using a DSC experiment, as depicted in Fig. 2.

According to the Method "A" of the Borchardt and Daniels procedure, the total peak area (ΔH) was divided into 20 equal intervals between the temperature that corresponds to 10% of the peak area and the temperature correspondent to 90% of the peak area, named $T_{10\%}$ and $T_{90\%}$. For each one of the 21 points (including extremes), the values of dH/dt and ΔH_T (corresponding to reaction rate and remaining heat of reaction, respectively), were estimated. Then, these values were used in Eqs. 4 and 5 to derive each da/dt and $[1 - \alpha]$ values,

which are the input data for the multiple linear regression data treatment (as described in ASTM E1970 [32]).

$$[1 - \alpha] = \frac{\Delta H_T}{\Delta H} \tag{4}$$

$$\frac{d\alpha}{dt} = \frac{dH}{dt} / \Delta H \tag{5}$$

The kinetic parameters, such as activation energy, Arrhenius pre-exponential factor, and reaction order, were then estimated using the data treatment proposed in the method ASTM E1970 [32]. Finally, from the plotting of Eq. 2, a straight line should be obtained using the reciprocal of absolute temperature (1/T), in the x-axis, versus the logarithm of the reaction rate constant (ln[k(T)]), in the y-axis. The slope of the straight line is equal to $-E/R$ and the intercept is equal to $\ln[Z]$. In addition, this plot also provides r and R^2 , which means the repeatability and reproducibility values, respectively. If both values are higher than 0.95 is an indication that the Borchardt and Daniels method is suitable for a given situation [16].

3 Results and discussion

The thermal profiles of the BB/CB blends are presented in Fig. 3. The curves are divided into three regions. The first exothermic peaks of each formulation are depicted in Region I, the second peaks in Region II and region III presents the higher temperature range ($T > 378^\circ\text{C}$). Since biodiesel is obtained from vegetable oils, the oxidative stability is the property that mostly affects its quality during extended storage time. Its thermoxidation may generate

compounds that could compromise the physicochemical properties and engine performance [33–36]. Therefore, an evaluation of thermal behavior, oxidation kinetic parameters, and quality improvement are important factors for reliable commercialization of biodiesel.

According to Thurgood et al. [13] and Micic et al. [14] the first peak is the main response of the DSC curve to evaluate the oxidation of a lipid compound. In other words, the hydroperoxide formation occurs in the first peak, representing the beginning of the oxidation reaction. The second peak is characterized by the decomposition of hydroperoxides, and finally, region III corresponds to the complete thermal deterioration of the sample. Our results are in accordance to Conceição et al. [37], in their work the calorimetric curve of castor oil biodiesel presented exothermic transitions attributed to the process of decomposition of esters on temperatures higher than 200°C .

In this context, among the DSC curve parameters established by the ASTM E537 standard, T_s of the first peak was chosen to determine the beginning of the oxidation reaction. The derivation of the other parameters of this standard, namely, ΔH , T_o and T_p , are depicted in Fig. 4 [12–14]. The ASTM E537 parameters of each formulation are then presented in Table 2.

Analyzing only the T_s of each formulation, it is possible to observe its increase with increasing castor content, as previously reported by Silva [38] for castor/sunflower and castor/soybean biodiesel blends using P-DSC. Indeed, biodiesels with similar fatty acids structures present the same T_s [39]. Additionally, Farias et al. [40] reported that castor oil enhanced the oxidative stability of the biodiesel blends because of the high content of ricinoleic acid.

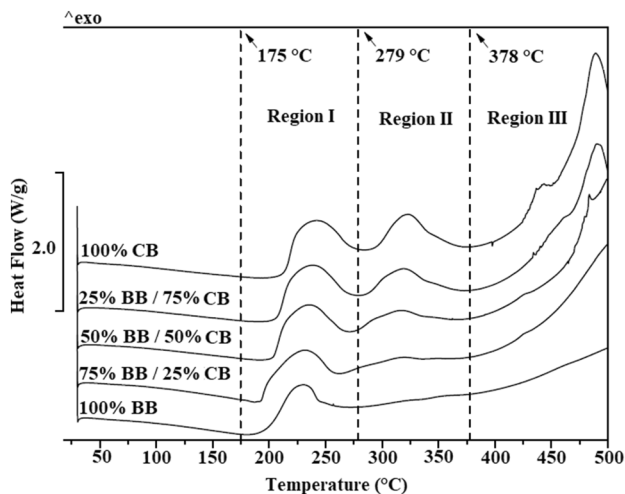


Fig. 3 Thermal profiles of BB/CB blends

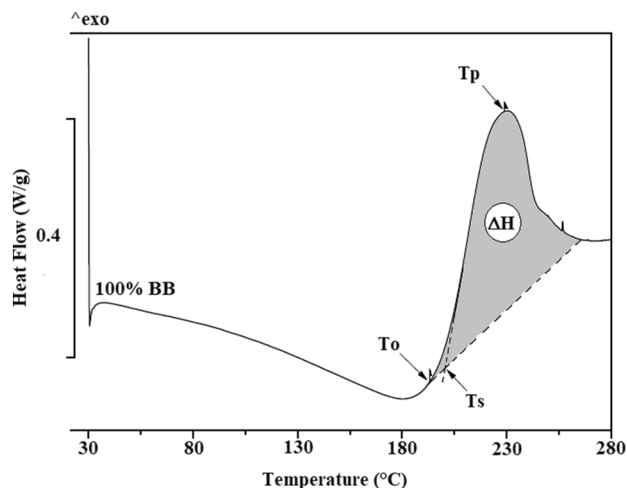


Fig. 4 Evaluation of DSC parameters of the first exothermic peak obtained using the ASTM E537 method

Table 2 DSC parameters estimated according to the ASTM E537 for CB/BB blends

Sample	β^a ($^{\circ}\text{C min}^{-1}$)	T_o^b ($^{\circ}\text{C}$)	T_s^c ($^{\circ}\text{C}$)	T_p^d ($^{\circ}\text{C}$)	ΔH^e (J g^{-1})
100% babassu	5	192.06	201.00	227.78	209.56
75% babassu 25% castor		193.30	193.46	228.10	275.75
50% babassu 50% castor		201.02	204.64	231.29	293.15
25% babassu 75% castor		200.34	208.30	234.37	327.47
100% castor		211.52	214.92	237.86	323.24

^a β —heating rate of DSC method^b T_o —onset temperature^c T_s —extrapolated onset temperature^d T_p —peak temperature^e ΔH —enthalpy variation**Table 3** Estimated kinetic parameters and R^2 for CB/BB blends according to ASTM E2041 and ASTM E1970 standards

Sample	n^a	E^b (kJ mol^{-1})	$\ln Z^c$ (Z, min^{-1})	R^2^d
100% babassu	1	114.03 ± 5.55	21.99 ± 1.33	0.9570
75% babassu 25% castor		109.12 ± 1.65	20.79 ± 0.40	0.9957
50% babassu 50% castor		102.70 ± 0.72	18.96 ± 0.17	0.9991
25% babassu 75% castor		97.62 ± 1.12	17.51 ± 0.26	0.9975
100% castor		96.15 ± 0.63	16.70 ± 0.15	0.9992

^a n —reaction order^b E —activation energy^c $\ln Z$ —logarithm of Arrhenius pre-exponential factor^d R^2 —reproducibility value

From Fig. 4 and Table 2, the exception of the adding CB to the growth in T_s was the sample containing 25% of castor biodiesel, which showed a lower T_s value than the pure babassu biodiesel sample. In summary, from the T_s analysis, the pure castor biodiesel sample is the most resistant to oxidation, while the 75/25 BB/CB formulation is more prone to oxidize.

Proceeding on the evaluation of the oxidative stability of the BB/CB blends, the determination of the kinetic parameters by ASTM E2041 may contribute to providing a deeper discussion. As mentioned, the data were collected from the DSC measurements using the recommendations of the ASTM E2041 method, and then statistically treated with the ASTM E1970 method. The estimated parameters are presented in Table 3.

The highest value of activation energy was observed for the pure babassu biodiesel sample ($114.03 \text{ kJ mol}^{-1}$), and the lowest value was observed for the pure castor biodiesel sample ($96.15 \text{ kJ mol}^{-1}$). Also, as the content of CB increases the activation energy increases, which is an indication that the oxidation reaction occurs more easily for CB than for BB. However, observing the results for induction periods (see Table 1), DSC parameters (Table 2), and the chemical structures of ricinoleic acid and lauric acid, CB is clearly more resistant to oxidation than BB.

Therefore, as suggested in other studies [13, 14], the reaction rate, $k(T)$, of the kinetic parameters, would be more suitable to evaluate the oxidative stability of lipid substances, including the BB/CB blends. The chosen temperature to calculate $k(T)$ was 485.15 K ($212 \text{ }^{\circ}\text{C}$) since the oxidation reaction is in progress for all blends at this temperature, even in different stages. The values obtained for $k(T)$ are shown in Table 4.

Observing the $k(T)$ results, pure castor biodiesel is clearly more resistant to oxidation with the lowest $k(T)$ value, $1.02 \times 10^{-3} \text{ min}^{-1}$. As the castor content decreases in the blends, the $k(T)$ values increase, indicating that the addition of CB improves the oxidative stability of the blend. Again, the exception is the 75/25 BB/CB blend, with $k(T)$ of $1.90 \times 10^{-3} \text{ min}^{-1}$, slightly higher than $1.88 \times 10^{-3} \text{ min}^{-1}$ of the pure babassu biodiesel. Additionally, it is possible to observe a pattern between the T_s values reported in Table 2 and the $k(T)$ values shown in Table 4. In other words, the pure castor biodiesel sample is the most resistant to oxidation, while the 75/25 BB/CB blend is more prone to oxidize.

From these results, similarly to what was previously reported by Santos et al. [28] in a DFT study, castor biodiesel may be used as an additive to improve the oxidative stability of biodiesel obtained from other sources, such as babassu.

Table 4 Values of reaction rate $k(T)$ at 485.15 K for CB/BB blends

Sample	100% babassu	75% babassu 25% castor	50% babassu 50% castor	25% babassu 75% castor	100% castor
$k(T), 485.15 \text{ K} (\text{min}^{-1})$	1.88×10^{-3}	1.90×10^{-3}	1.51×10^{-3}	1.24×10^{-3}	1.02×10^{-3}

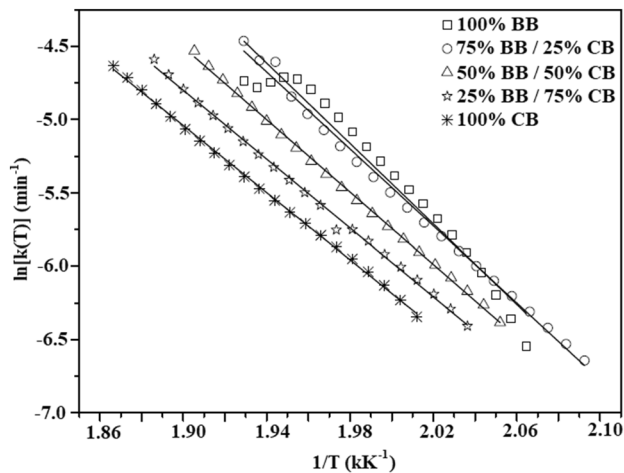


Fig. 5 Plot of $1/T$ versus $\ln[k(T)]$ for all BB/CB blends

However, without any supplementary tests, it is not clear the reason why the 75/25 BB/CB blend presented higher susceptibility to oxidize than the pure babassu biodiesel sample, but this suggests that there is some synergy effect or other factors involved in the biodiesel oxidation reactions, promoting this unexpected result.

Finally, the plot of $1/T$ versus $\ln[k(T)]$ is illustrated in Fig. 5, as a result of the application of both ASTM E2041 and ASTM E1970 standards.

From Fig. 5 and Table 4, it is possible to realize that most of the samples presented good approximation of a straight line, showing R^2 values higher than 0.9900. In general, the statistical model offered an accurate fitting of the experimental data with the Arrhenius equation [16].

The DSC results indicate that this technique may be used to monitor the thermoxidation of biodiesel since they are in agreement with previous reports on biodiesel oxidation using the Rancimat method [35–42].

4 Conclusions

Binary blends of babassu and castor biodiesel samples were prepared, in proportions of babassu/castor mass ratios of 0/100, 25/75, 50/50, 75/25, and 100/0, in order to evaluate their oxidative behavior. The biodiesel properties depend on their esters. Because of this, the babassu and castor biodiesel samples, evaluated using DSC, showed different thermoxidative stabilities. The sample with the highest thermoxidative stability was the pure castor biodiesel showing the highest value of extrapolated onset temperature (T_o) and the lowest value of $k(T)$, while the 75/25 BB/CB binary blend presented the worst oxidative stability behavior. Therefore, we conclude that castor biodiesel may improve the oxidative

stability of babassu biodiesel, and the DSC technique may be used for assessing, monitoring, and ascertaining the oxidation kinetic parameters and mapping the thermal stability of biodiesel blends prepared from those two vegetable oils. In addition, the high R^2 values imply that the use of Borchardt–Daniels method is suitable to evaluate the oxidation reaction of biodiesel samples, and the results indicate that this technique may be used to monitor the thermoxidation of biodiesel since it shows good agreement with previous reports using the Rancimat method.

Acknowledgements The authors acknowledge CNPq (406697/2013-2 and 308280/2017-2), CAPES, FINEP, and FUNCAP (Process AEP-0128-00220.01.00/17) for financial support.

Compliance with ethical standards

Conflict of interest On behalf of all authors, the corresponding author states that there is no conflict of interest.

References

- Nabora CS, Kingondu CK, Kiveveli TT (2019) *Tamarindus Indica* fruit shell ash: a low cost and effective catalyst for biodiesel production from *Parinari curatellifolia* seeds oil. SN Appl Sci 1:253. <https://doi.org/10.1007/s42452-019-0256-3>
- Phukan MM, Bora P, Gogoi K, Konwar BK (2019) Biodiesel from *Saccharomyces cerevisiae*: fuel property analysis and comparative economics. SN Appl Sci 1:153. <https://doi.org/10.1007/s42452-019-0159-3>
- Hajilari N, Rezakazemi M, Shirazian S (2019) Biofuel types and membrane separation. Environ Chem Lett 17:1–18. <https://doi.org/10.1007/s10311-018-0777-9>
- Brazilian Energy Balance 2017 (2016) Empresa de Pesquisa Energética. Rio de Janeiro: EPE, 2017
- Santya G, Maheswaran T, Yee KF (2019) Optimization of biodiesel production from high free fatty acid river catfish oil (*Pangasius hypophthalmus*) and waste cooking oil catalyzed by waste chicken egg shells derived catalyst. SN Appl Sci 1:152. <https://doi.org/10.1007/s42452-018-0155-z>
- Rios MAS, Santos FFP, Maia FJN, Mazzetto SE (2013) Evaluation of antioxidants on the thermo-oxidative stability of soybean biodiesel. J Therm Anal Calorim 112:921–927
- Akhtar T, Tariq MI, Iqbal S, Sultana N, Wei CK (2017) Production and characterization of biodiesel from *Eriobotrya Japonica* seed oil: an optimization study. Int J Green Energy 14:569–574
- Gharehghani A, Mirsalim M, Hosseini R (2017) Effects of waste fish oil biodiesel on diesel engine combustion characteristics and emission. Renew Energy 101:930–936
- Yusuff AS, Lala MA, Popoola LT, Adesina OA (2019) Optimization of oil extraction from *Leucaena leucocephala* seed as an alternative low-grade feedstock for biodiesel production. SN Appl Sci 1:357. <https://doi.org/10.1007/s42452-019-0364-0>
- Lôbo IP, Ferreira IP, Cruz RS (2009) Biodiesel: parâmetros de qualidade e métodos analíticos. Quim Nova 32:1596–1608
- Taylor SM, Fryer PJ (1993) The suitability of DSC to obtain thermal reaction kinetics of whey proteins. Food Hydrocoll 6:543–557

12. Kok MV, Varfolomeev MA, Nurgaliev DK (2019) Thermal characterization of crude oils by pressurized differential scanning calorimeter. *J Pet Sci Eng* 177:540–543
13. Thurgood J, Ward R, Martini S (2007) Oxidation kinetics of soybean oil/anhydrous milk fat blends: a differential scanning calorimetry study. *Food Res Int* 40:1030–1037. <https://doi.org/10.1016/j.foodres.2007.05.004>
14. Micic DM, Ostojic SB, Simonovic MB, Krstic G, Pezo LL, Simonovic BR (2015) Kinetics of blackberry and raspberry seed oils oxidation by DSC. *Thermochim Acta* 601:39–44
15. ASTM E537–12 (2012) Standard test method for the thermal stability of chemicals by differential scanning calorimetry. ASTM International, West Conshohocken. <https://doi.org/10.1520/E0537-12>
16. ASTM E2041–13 (2018) Standard test method for estimating kinetic parameters by differential scanning calorimeter using the Borchardt and Daniels method. ASTM International, West Conshohocken. <https://doi.org/10.1520/E2041-13E01>
17. Souza FHN, Maia FJN, Mazzetto SE, Nascimento TL, Andrade N (2013) Oxidative stability of soybean biodiesel in mixture with antioxidants by thermogravimetry and rancimat method. *Chem Biochem Eng Q* 27:327–334
18. Souza FHN, Almeida LR, Batista FSCL, Rios MAS (2011) UV-visible spectroscopy study of oxidative degradation of sunflower biodiesel. *Energy Sci Technol* 2:56–61
19. Rodrigues JS, Valle CP, Guerra PAGP, Rios MAS, Malveira JQ, Ricardo NMPS (2017) Study of kinetics and thermodynamic parameters of the degradation process of biodiesel produced from fish viscera oil. *Fuel Process Technol* 161:95–100
20. Okwundu OS, El-Shazly AH, Elkady M (2019) Comparative effect of reaction time on biodiesel production from low free fatty acid beef tallow: a definition of product yield. *SN Appl Sci* 1:140. <https://doi.org/10.1007/s42452-018-0145-1>
21. EN 14103: Fat and oil derivatives—fatty acid methyl esters (FAME)—determination of ester and linolenic acid methyl esters content
22. ASTM D7042–16e3 (2016) Standard test method for dynamic viscosity and density of liquids by stabinger viscometer (and the calculation of kinematic viscosity). ASTM International, West Conshohocken
23. ASTM D445–18 (2018) Standard test method for kinematic viscosity of transparent and opaque liquids (and calculation of dynamic viscosity). ASTM International, West Conshohocken
24. EN 14104: Fat and oil derivatives—fatty acid methyl esters (FAME)—determination of acid value
25. EN 14112: Fat and oil derivatives—fatty acid methyl esters (FAME)—determination of oxidation stability (accelerated oxidation test)
26. Resolution no 45/2014 (2014) National agency of petroleum, natural gas and biofuels (ANP). <http://legislacao.anp.gov.br/?path=legislacao-anp/resol-anp/2014/agosto&item=rnp-45-2014>. Accessed 18 Dec 2018
27. Knothe G, Razon LF (2017) Biodiesel fuels. *Prog Energy Combust Sci* 58:36–59
28. Santos VML, Silva JAB, Stragevitch L, Longo RL (2011) Thermochemistry of biodiesel oxidation reactions: a DFT study. *Fuel* 90:811–817
29. Zuleta EC, Rios LA, Benjumea PN (2012) Oxidative stability and cold flow behavior of palm, sacha-indi, jatropha and castor oil biodiesel blends. *Fuel Process Technol* 102:96–101
30. ASTM E967–08 (2014) Standard test method for temperature calibration of differential scanning calorimeters and differential thermal analyzers. ASTM International, West Conshohocken. <https://doi.org/10.1520/e0967>
31. ASTM E968–02 (2014) Standard practice for heat flow calibration of differential scanning calorimeters. ASTM International, West Conshohocken. <https://doi.org/10.1520/e0968>
32. ASTM E1970–16 (2016) Standard practice for statistical treatment of thermoanalytical data. ASTM International, West Conshohocken. <https://doi.org/10.1520/e1970-16>
33. Joelianingsih H, Maeda S, Hagiwara H, Nabetani Y, Sagara TH, Soerawidjaya AH, Tambunan K, Abdullah K (2008) Biodiesel fuels from palm oil via the non-catalytic transesterification in a bubble column reactor at atmospheric pressure: a kinetic study. *Renew Energy* 33:1629–1636
34. Pullen J, Saeed K (2012) An overview of biodiesel oxidation stability. *Renew Sustain Energy Rev* 16:5924–5950
35. Santos AGD, Souza LD, Caldeira VPS, Farias MF, Fernandes VJ, Araujo AS (2014) Kinetic study and thermoxidative degradation of palm oil and biodiesel. *Thermochim Acta* 592:18–22
36. Araújo SV, Rocha BS, Luna FMT, Rola EM, Azevedo DCS, Cavalcante CL Jr (2011) FTIR assessment of the oxidation process of castor oil FAME submitted to PetroOXY and Rancimat methods. *Fuel Process Technol* 92:1152–1155
37. Conceição MM, Candeia RA, Silva FC, Bezerra AF, Fernandes VJ, Souza AG (2007) Thermoanalytical characterization of castor oil biodiesel. *Renew Sustain Energy Rev* 11:964–975
38. Silva HKTA (2014) Estudo da influência do biodiesel de mamona como aditivo antioxidante para o biodiesel de girassol e soja. Dissertation, Universidade Federal do Rio Grande do Norte
39. Galvao LPFC, Santos AGD, Gondim AD, Barbosa MN, Araujo AS, Souza L, Fernandes VJ (2011) Comparative study of oxidative stability of sunflower and cotton biodiesel through P-DSC. *J Therm Anal Calorim* 106:625–629. <https://doi.org/10.1007/s10973-011-1411-2>
40. Farias RMC, Conceição MM, Candeia RA, Silva MCD, Fernandes VJ, Souza AG (2011) Evaluation of the thermal stability of biodiesel blends of castor oil and passion fruit. *J Therm Anal Calorim* 106:651–655. <https://doi.org/10.1007/s10973-011-1566-x>
41. Melo MAMF, Melo MAR, Pontes ASGC, Farias AFF, Dantas MB, Calixto CDC, Souza AG, Carvalho Filho JR (2014) Non-conventional oils for biodiesel production: a study of thermal and oxidative stability. *J Therm Anal Calorim* 117:845–849
42. Miranda MIG, Samios D, Piñeiro TO, Vagheti JCP, Piatnicki CMS (2017) Kinetics of oxidation and decomposition of soybean biodiesel evaluated by the TTT superposition theory and the Freeman–Carroll method. *J Mol Liq* 245:121–128

Publisher's Note Springer Nature remains neutral with regard to jurisdictional claims in published maps and institutional affiliations.